Optical tweezers for studying taxis in parasites

Article *in* Journal of Optics · March 2011

DOI: 10.1088/2040-8978/13/4/044015

13 authors, including:

André De Thomaz
University of Campinas
77 PUBLICATIONS **563** CITATIONS
SEE PROFILE

Adriana Fontes
Federal University of Pernambuco
176 PUBLICATIONS **1,502** CITATIONS
SEE PROFILE

Cecilia Stahl Vieira
Fundação Oswaldo Cruz
25 PUBLICATIONS **263** CITATIONS
SEE PROFILE

Liliana de Ysasa Pozzo
University of São Paulo
12 PUBLICATIONS **153** CITATIONS
SEE PROFILE

Optical tweezers for studying taxis in parasites

2011 J. Opt. 13 044015

(http://iopscience.iop.org/2040-8986/13/4/044015)

IOP Publishing Journal of Optics
J. Opt. **13** (2011) 044015 (7pp) doi:10.1088/2040-8978/13/4/044015

Optical tweezers for studying taxis in parasites

A A de Thomaz[1], A Fontes[2], C V Stahl[3], L Y Pozzo[1], D C Ayres[4], D B Almeida[1], P M A Farias[2], B S Santos[5], J Santos-Mallet[3], S A O Gomes[3], S Giorgio[4], D Feder[6] and C L Cesar[1]

[1] Departamento de Eletrônica Quântica, Instituto de Física, Universidade Estadual de Campinas (UNICAMP), Campinas-SP, Brazil
[2] Departamento de Biofísica e Radiobiologia, Centro de Ciências Biológicas, Universidade Federal de Pernambuco (UFPE), Recife-PE, Brazil
[3] Laboratório de Transmissores de Leishmanioses, Setor de Entomologia Médica e Forense, IOC-FIOCRUZ, Rio de Janeiro-RJ, Brazil
[4] Departamento de Parasitologia, Instituto de Biologia, Universidade Estadual de Campinas (UNICAMP), Campinas-SP, Brazil
[5] Departamento de Ciências Farmacêuticas, Centro de Ciências da Saúde, Universidade Federal de Pernambuco (UFPE), Recife-PE, Brazil
[6] Laboratório de Biologia de Insetos, Universidade Federal Fluminense (UFF), Rio de Janeiro-RJ, Brazil

E-mail: athomaz@ifi.unicamp.br

Received 4 May 2010, accepted for publication 1 September 2010
Published 4 March 2011
Online at stacks.iop.org/JOpt/13/044015

Abstract
In this work we present a methodology to measure force strengths and directions of living parasites with an optical tweezers setup. These measurements were used to study the parasites chemotaxis in real time. We observed behavior and measured the force of: (i) *Leishmania amazonensis* in the presence of two glucose gradients; (ii) *Trypanosoma cruzi* in the vicinity of the digestive system walls, and (iii) *Trypanosoma rangeli* in the vicinity of salivary glands as a function of distance. Our results clearly show a chemotactic behavior in every case. This methodology can be used to study any type of taxis, such as chemotaxis, osmotaxis, thermotaxis, phototaxis, of any kind of living microorganisms. These studies can help us to understand the microorganism sensory systems and their response function to these gradients.

Keywords: optical tweezers, chemotaxis, taxis, *Trypanosoma cruzi*, *Trypanosoma rangeli*, *Leishmania amazonensis*, parasite–host interaction

1. Introduction

A fundamental goal of parasitology is the complete understanding of host–parasite interactions, such as Chagas disease caused by *Trypanosoma cruzi* (*T. cruzi*) and tegumentar leishmaniasis disease caused by *Leishmania amazonensis* (*L. amazonensis*). Chagas disease is present in over 15 countries in the Americas, with a prevalence of 13 million, with 3.0–3.3 million symptomatic cases and an annual incidence of 200 000 cases [1]. Leishmaniasis is another serious tropical disease that affects about 30 million people in Africa, the Middle East, and Central and South America [2]. Closely related but nonpathogenic to humans, *Trypanosoma rangeli* (*T. rangeli*), has a sympatric distribution with *T. cruzi*, and has the same vector. Antigenic similarity between *T. cruzi* and *T. rangeli* showed a serological cross-reactivity in human infection leading to a wrong diagnosis of Chagas disease [3].

The process where cells and microorganisms direct their movements according to certain gradients in their environment is known as taxis. They can sense and respond to temperature, osmotic pressure, light, chemicals, and other parameter gradients involved in their survival. When these biological systems direct their movements according to chemicals gradients, the process is called chemotaxis. Chemotaxis is the way that microorganisms find nutrients (for example, glucose), by swimming towards the highest concentration

of nourishment molecules, or to move away from poisons (for example, phenol) [4]. There are reports suggesting that spermatozoa use chemotaxis to direct their movement towards the ovum during fertilization. Sperm chemotaxis is a chemical guiding mechanism that may orient spermatozoa to the egg surface [5]. This mechanism is mediated by steroidal hormones and seems to depend on the production of reactive oxygen species (ROS) [5, 6]. Even for multicellular organisms, chemotaxis drives subsequent phases of development such as neuron and lymphocyte migration [7]. In addition, it has been recognized that chemotactic migration decreases during cancer metastasis [8]. Cell signalization is responsible for the chemotactic activity and many chemical receptors present mostly on cell membrane are involved in this kind of taxis [9].

There are many studies in the literature on chemotaxis, and other kinds of taxis, such as osmotaxis, performed by cells and microorganisms. Chemotaxis, for example, has been extensively studied from two points of view: (1) a black box point of view where the response is observed as a function of the stimulus and (2) a biochemical point of view where the biochemical reactions triggered by the receptors are observed [10–12]. The majority of the work on chemotaxis is on leukocytes, which have a kind of slow taxis based on crawling movement, unlike the taxis performed by bacteria and protozoa [13–15]. There are more studies on the chemotaxis of bacteria than protozoa [16–18]. The most commonly used method, the capillary assay, first created by Pfeffer [19] and later improved by Adler [20], is used for quantitative analysis. However, the measurements are based only on the number of cells found near the end of the higher concentration gradient capillary. Another methodology, introduced by Barros [18] to study the leishmania chemotaxis was based on measurement of the mean time of straight line movement. Movement in a straight line is defined here as the absence of abrupt changes of direction.

We propose a methodology to study biological systems taxis in real time using an optical tweezers setup. Optical tweezers is a very sensitive tool, based on photon momentum transfer, for individual, cell by cell, manipulation and measurements. It can be used to perform real time measurements of the force vectors, strength and direction, of living cells under chemical or other kinds of gradients [21]. This seems to be the ideal tool to perform observations of taxis response with high sensitivity to capture instantaneous responses to a given stimulus. Forces involved in the movement of unicellular parasites are very small, in the femto–piconewton range, about the same order of magnitude as the forces created in an optical tweezers. This methodology can provide real time information because the parasites can move the bead every ∼0.1 s and the detection is done every 0.5 μs. In the limit of low Reynolds numbers we can ignore inertia and the force can be calculated by the viscosity term:

$$6\pi\eta a\frac{\mathrm{d}x}{\mathrm{d}t} = F -> \Delta t = \frac{(6\pi\eta a)\Delta x}{F} \qquad (1)$$

assuming the viscosity (η) as water the viscosity, a (bead radius) as 4.5 μm, Δx (bead displacement) as 0.3 μm and F (force) as 0.3 pN, we found ΔT as ∼0.1 s.

To establish the methodology, we first investigated *L. amazonensis* flagellum impulse forces under one-dimensional stationary glucose gradients [21]. Subsequently, we applied a similar methodology to study chemotaxis of *T. cruzi* under distinct situations (see section 2). In this context, interaction studies of *T. cruzi* and insect gut molecules are important for a better understanding of this parasite life cycle [22]. One of the fundamental steps of the life cycle of *T. cruzi* in the invertebrate host occurs in the midgut of the triatomine vectors. Epimastigote forms of *T. cruzi* bind to perimicrovillar membrane (PMM), a physical and physiological barrier located in the midgut cells, and suffer intense multiplication. This process involves the recognition of glycomolecules and some hydrophobic proteins located on the surface of epimastigotes forms of *T. cruzi*. Chemotactic molecules as proteins/carbohydrates on PMM, have contributed to the adhesion and development of trypanosomes (epimastigotes forms) in the midgut of the invertebrate host [23–25]. Other trypanosomatid, *T. rangeli* (transmitted by saliva to a vertebrate host) needs to join the salivary glands of the insect vector to invade them and complete their life cycle in the invertebrate host [26]. Antigenic similarity between *T. cruzi* and *T. rangeli* has shown a serological cross-reactivity in human infection leading a misdiagnosis of Chagas disease [3]. *Rhodnius prolixus* (*R. prolixus*) is the second most important triatomine vector of Chagas disease due to its efficient adaptation to the human domicile. This vector has a strictly hematophagous behavior that makes these insects potential transmitters of many pathogens, including *T. cruzi* and *T. rangeli*, which is apparently harmless to humans but can be pathogenic to the insect vector [27]. We believe that the studies performed with *L. amazonensis* nicely complement *T. cruzi* and *T. rangeli* studies. The *L. amazonensis* work was performed in a very controlled situation, with a well known gradient strength and direction, while in the trypanosomes experiment the behavior of the parasite in the vicinity of the cell walls of its target tissues was observed. This methodology can be very useful to understand real biology, and is a demonstration that optical tweezers can provide valuable information in real situations. We believe also that the measurements performed by this system provided a better understanding of parasite cell biology, life cycles, and taxis. For a better understanding of taxis it is necessary to know not only the sense and direction of the parasite's movements but also their intensity.

2. Material and methods

Figure 1 shows the optical tweezers consisting of a Nd:YAG laser (Spectra Physics, model 3800S) strongly focused through a 100× oil immersion objective (NA > 1.25) of a microscope (Olympus BH2) equipped with a CCD camera and an x–y–z motorized stage (Prior Scientific, model ProScan, Rockland, Massachusetts, USA) controlled by a computer or a joystick. The propulsion forces of the protozoan flagellum were measured by the displacement of a polystyrene bead connected to the parasite trapped with an optical tweezers. The bead was connected to the parasite by non-specific agglutination. In the beginning of the movement, soon after

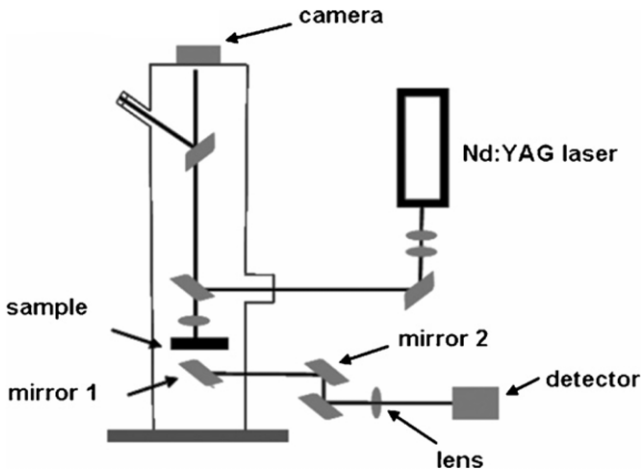

Figure 1. Experimental optical tweezers setup used for taxis studies [21].

the coupling with the bead, the microsphere can hinder a little the parasite movement, because sometimes the parasite stays above the bead. But, 1 min after the coupling, the parasite stays connected to the bead by the tip of the body or by a filament projection of the body membrane. After reaching this configuration, we started the acquisition. For these measurements we use a 9 μm diameter bead to avoid light scattering from the parasite itself and not from the bead. The x and y displacements of the bead were obtained by measuring the scattered light of the optical tweezers laser with a quadrant detector (QP506SD2—Pacific Sensor Incorporated). The quadrant detector was positioned in the back focal plane of the microscope with a 5 cm long focal distance lens to control the beam size on the detector. The signals were collected with an oscilloscope (Tektronix, model TDS 1012). The calibration was made by moving a fixed polystyrene bead in the x and y directions using a microscope translation [21].

2.1. Force calibration

We assumed a geometrical optics model to calibrate the force as a function of the bead displacement from the equilibrium position. The first step to calculate the optical force is to know the force that one ray performs on a bead (considering refractions and reflections). The forces of one ray for each direction (parallel and perpendicular to the incident ray) are given by:

$$F_{z'} = \frac{n_1 P}{c}\left[1 - R\cos(\pi + 2\sigma) + \sum_{n=0}^{\infty} T^2 R^n \cos(\alpha + n\beta)\right]$$
$$F_{y'} = \frac{n_1 P}{c}\left[-R\sin(\pi + 2\sigma) + \sum_{n=0}^{\infty} T^2 R^n \sin(\alpha + n\beta)\right]. \quad (2)$$

The trick to perform the sums is to change to the complex plane by the transformation $F_c = F_{z'} + \mathrm{i}F_{y'}$, so the series become a geometric series, and the result for F_c is:

$$F_c = \frac{n_1 P}{c}\left(1 + R\exp(2\sigma\mathrm{i}) - T^2\exp(\mathrm{i}\alpha)\left[\frac{1}{1 - R\exp(\mathrm{i}\beta)}\right]\right) \quad (3)$$

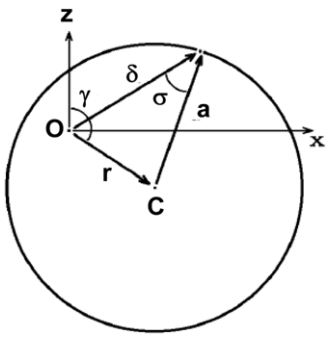

Figure 2. Change in the coordinates' origin and definition of the angle and vectors used.

where $\alpha = 2(\sigma - x)$, $\beta = (\pi - 2x)$, and $\sin x = n\sin\sigma$. The variable σ is the incident angle, $n = n_1/n_2$ is the relative refraction index between the fluid (n_1) and the sphere (n_2), c is the light velocity and P is the laser power. The variables $R = (\tan(\sigma - x)/\tan(\sigma + x))^2$ and $T = 1 - R$ are the reflectance and transmittance, respectively, for a linear polarized ray. This expression depends on the value of the incidence angle σ and the relative refractive index. The incidence angle varies for each ray so it is necessary to change the origin of the coordinates to a fixed position which we choose as the focus of the beam, as shown in figure 2. By writing the incidence angle σ as function of the angle γ and the vectors $\boldsymbol{\delta}$ and $\mathbf{r}$, the final expression of the force will depend only on the displacement $\mathbf{r}$ vector, connecting the beam focus to the center of the sphere, the convergence angle of the beam (numerical aperture), the sphere radius, beam power (supposed to be equal for each ray), and the relative refraction index, which are all measurable or known parameters. Using the cosine law for the vector, this transformation is given by: $\sigma = \arccos(1 + d^2 - (r/a)^2/2d)$, where $d = \|\vec{\delta}\|$ and the displacement $\vec{r} = (r\sin\gamma, 0, r\cos\gamma)$.

The force vector for the whole conic beam is obtained by integration, $F = \int \vec{F}\,\mathrm{d}A / \int \mathrm{d}A$, where the area element is given by $\mathrm{d}A = \sin\theta\cos\theta\,\mathrm{d}\theta\,\mathrm{d}\varphi$ obtained using the Abbe sine condition, the angle θ varies from $0 \leqslant \theta \leqslant \theta_{\max}$, the maximum-convergence-objective-angle, the azimuthal angle varies from $0 \leqslant \varphi \leqslant 2\pi$.

The expression for the optical force obtained above was checked against a hydrodynamic force on a particle dragged at known velocities in a Neubauer chamber, which has two walls 100 μm apart. The presence of the walls means that we cannot just use Stokes' law. The dragging force on a sphere in the vicinity of two walls can be found in [28] by using an infinite series of images. The dragging force is given by, neglecting terms of order higher than $(a/l)^3$:

$$F = \frac{6\pi\eta a u}{1 - A(\frac{a}{l}) + B(\frac{a}{l})^3 + \cdots}. \quad (4)$$

Here, u and a are the sphere velocity and its radius, η is the fluid viscosity and l is the distance from the center of the sphere to the bottom of the chamber. The constants A and B are complicated numerical integrals that depend on l and b, where b is the distance from the center of the sphere to the cover slip. Both, the expression for the hydrodynamic and optical force

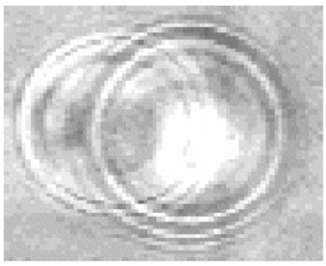

Figure 3. Experimental displacement of a sphere at null and constant velocities.

were numerically obtained by using the software Mathematica (Wolfram Research).

We experimentally checked our model results using 9 μm diameter polystyrene spheres (Polysciences). At null velocity there are no optical or hydrodynamic forces actuating on the sphere, except for a small force due to the reflections, which do not change its lateral position, so the center of the sphere coincides with the laser focus. On the other hand, at a constant velocity, the optical force will equilibrate the hydrodynamic one through a change in the center position of the sphere that is no longer in the beam focus. This displacement can be easily measured by superimposing the images before and after the dragging and measuring the distance between the centers as shown in figure 3.

The movement of the microspheres was recorded on tape, then digitized using a video capture card and the displacement was measured with the software Image-Pro Plus (Media Cybernetics). Because the movement is in the x direction we assume the γ angle to be 90°. The depth l of 15, 25, 50, 75, and 85 μm were chosen and measured using the microscope micrometer, while b is obtained from the difference in the total depth of 100 μm of our Neubauer chamber. A microcomputer controls translation stage drag velocities that we set to 150, 200, 250, 300, and 350 μm s^{-1}. The optical power was measured after the microscope objective using a spectralon integrating sphere (Labsphere). The fluid refraction indexes and viscosities were varied together by using solutions of water and sugar at 14%, 20%, and 28% concentrations. We checked the handbook values of the solution with an Ostwald viscometer and an Abbe refractometer.

With this experimental scheme we have been able to change, for a given optical power the following parameters: the dragging velocity, the depth l, the viscosity η and the relative refractive index n. Knowing all the parameters, we were able to calculate both the hydrodynamic and the optical forces, and we could compare both forces for a large range of different parameters. Figure 4 shows a plot of the calculated optical versus hydrodynamic forces for more than 30 points. The slope of the straight line is 1.07, very close to the expected slope of 1 and the R^2 value is higher than 0.9. This small difference can easily be explained by systematic error of the polystyrene sphere refractive index provided by the manufacturer. This plot shows the ability of our procedure to measure forces in the hundreds of piconewtons scale.

We also dragged the spheres at the same velocities in a solution of 20% and 32% glycerol in water to measure its

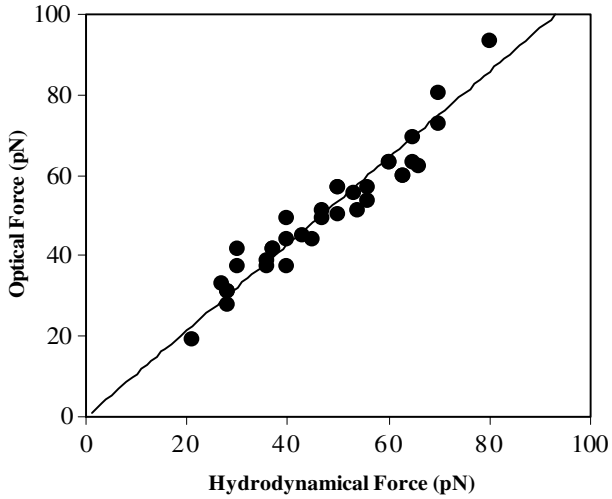

Figure 4. Plot of the optical versus hydrodynamic force for a wide range of parameters.

Table 1. Fluid viscosities tabled in the *Handbook of Chemistry and Physics* and measured by optical tweezers.

	20%	32%
Handbook's values	1.73 cP	2.63 cP
Our values	1.83 cP ± 5%	2.76 cP ± 5%

viscosity, as shown in table 1 and compared our result with the *Handbook of Chemistry and Physics* values [29]. These values confirm again the precision of our models. We only needed 10 μl of the fluid to measure these viscosities using optical tweezers, showing the ability of this technique to measure local viscosity of very small amounts of biological fluids.

The displacement of the bead due to the parasite's flagellum propulsion was then measured to determine the numerical values for the optical force and, consequently, for the force of the parasite.

For *L. amazonensis* measurements, we developed a chamber in order to create a stationary concentration gradient. The gradient was obtained by connecting two large reservoirs with a tiny duct capable of keeping the chemical gradient constant for more than 10 h. The size of the duct was: $\delta = 100$ μm, $L = 2.6$ cm, $w = 0.3$ cm—where δ is the depth, L is the length and w is the width. We observed the behavior of the same protozoan *L. amazonensis* in real time under two glucose gradients (0.2 and 0.5%). For the measurements we add 20 μl of the culture medium solution with the parasites to reservoir 1 and 20 μl of the culture medium with glucose only to the other reservoir (reservoir 2).

For *T. cruzi* measurements we just used an ordinary Neubauer chamber containing: (i) parasites or (ii) parasites plus slices of midgut of *R. prolixus* (invertebrate parasite host), (iii) parasites plus hindgut of *R. prolixus* (metacyclogenesis site), and (iv) slices of salivary gland without the perimicrovillar membrane. By trapping and moving *T. cruzi*, we measure the movements of the parasite away from the gut walls, in the vicinity of midgut cells and in the vicinity of hindgut and salivary gland cells. For this case the system used was similar

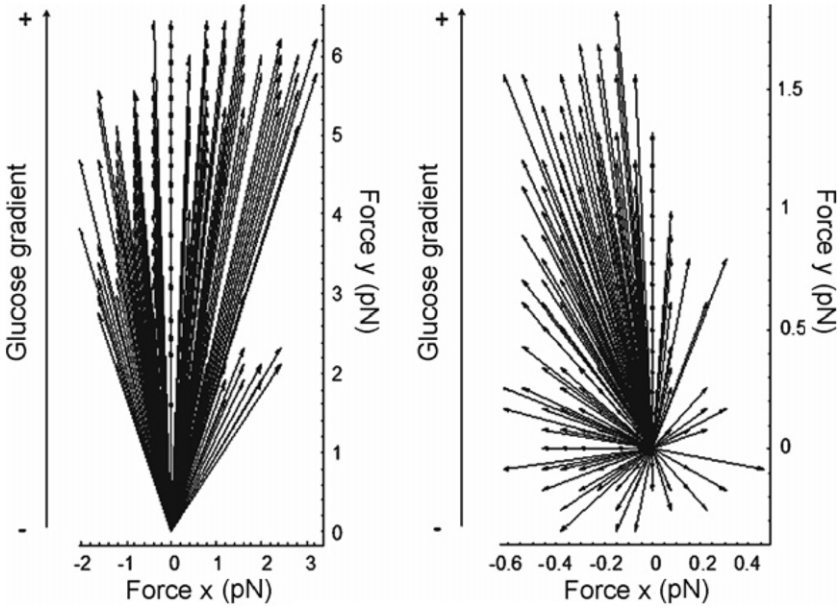

Figure 5. Bidimensional vector force plot for 0.5% (left) and 0.2% (right) glucose gradients [21].

to the system used in the case of *L. amazonensis*. The only differences are the microscope that is now an IX-81 Olympus inverted microscope, and the objective lens, a 60× 1.3 NA. Another calibration of the quadrant detector was made and forces were calculated in the same way.

3. Results

Figure 5 shows the plot of the vector force (for 0.5% and 0.2%) with a clear directionality towards the gradient. Without the gradient the parasites show only erratic movement. These results suggest that both, force strength and direction, are used by the parasites to perform chemotaxis. The force sensitivity of the optical tweezer system can go down to forces as small as 100 fN, much smaller than the noise force variations of the parasites. However, the sensitivity for gradient concentration depends on the parasites and the chemical substance. From figure 5, one can observe that for larger gradients, the forces are larger and the movement is more directed.

In order to sense these gradients the parasites started to swim around in circles four or five times, which could be an effective way to sense the gradients of a region much larger than the parasite itself. Figure 6 shows four pictures of this behavior of *L. amazonensis*.

For *T. cruzi* measurements, we first observed the behavior of the parasite more than 50 μm away from the midgut cells. In this case it just showed an erratic movement. The force directions were distributed randomly and the maximum strength was 0.8 pN. Figure 7(a) shows the plot of the vector force for this situation. The same erratic movement was observed when the parasite was in contact with the hindgut and salivary gland cells, figures 7(b) and (c).

On the other hand, less than 20 μm away from the midgut cells we observed a change in the behavior of the parasite. Figure 8(a) shows the parasite projecting its flagellum towards

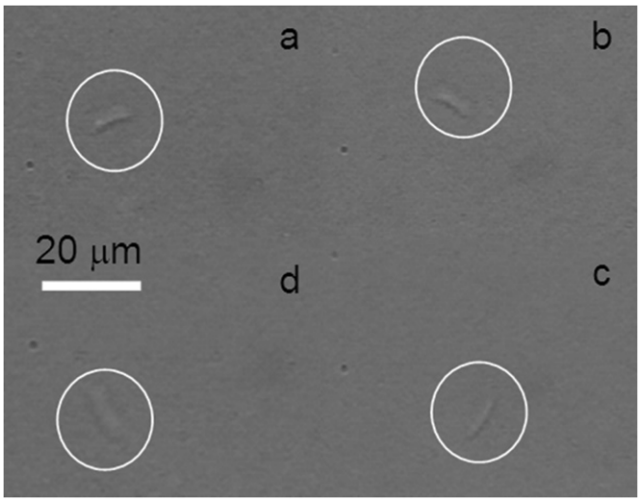

Figure 6. *L. amazonensis* swimming in circles to sense the glucose gradient. Four pictures of the whole movement are shown [21].

the cells. Figure 8(b) shows the force vectors in the presence of midgut cells. There are variations both in the strength and direction of the forces compared to the movement of the *T. cruzi* alone. It is possible to observe in the vectors of figure 8 that there is an effort of the parasite to swim towards the midgut cells. The maximum strength is, in this case, 0.8 pN. This result contrasts with the result of *L. amazonensis* that exerts higher forces in the presence of a steeper gradient. But if we observe the values of the forces in figure 7(a), we notice that there are maximum forces of 0.8 pN in the positive vertical direction but it is 0.6 pN in the negative direction. Now, in figure 8(b) there are forces up to 1.0 pN in the direction of the cells but forces as low as 0.4 pN in the other direction. The measurements of the forces were performed in different parasites, taking this into account we cannot analyze the forces by absolute values

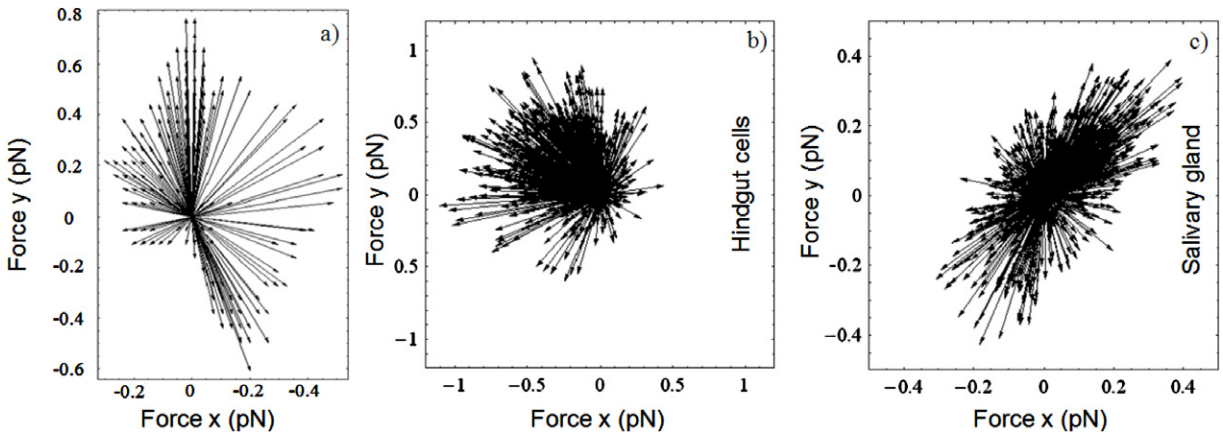

Figure 7. (a) Bidimensional vector force plot for *T. cruzi* without the presence of any chemical gradient. Bidimensional vector force plot for *T. cruzi* in the presence of hindgut cells (b) and salivary gland (c).

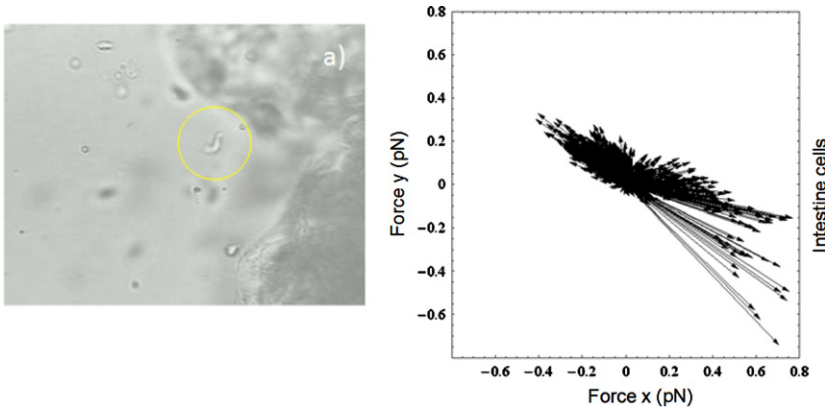

Figure 8. (a) Picture showing *T. cruzi* (inside the circle) projecting its flagellum towards the cells at the right [30]. The gradient is being generated by all cells. (b) Bidimensional vector force plot of *T. cruzi* in the presence of intestine cells.

but by relative values in the same graph. Furthermore we are observing graphs of different species of parasites under different conditions. In the case of *L. amazonensis* the direction and the value of the gradient can be controlled, the forces can be measured in the same parasite, alone and in the presence of the gradient. We cannot do that with *T. cruzi*, if we use the intestine cells to generate the gradient.

The same strategy to sense the gradient in the *L. amazonensis* case was observed in the *T. cruzi* case. *T. cruzi* swims around in circles in order to verify several points of the gradient and then takes the decision about the direction of the higher concentration of the attractive substance.

The result for *T. rangeli* is presented in figure 9 below. The trapped parasite was moved close to the salivary gland, its binding site, and the forces were measured. The directionality arises again and it is possible to see the higher force vectors pointing in the direction of the salivary gland. The same strategy to sense the gradient was observed again. The parasites swim in circles before going specifically to the direction of higher concentration of the attractive substance.

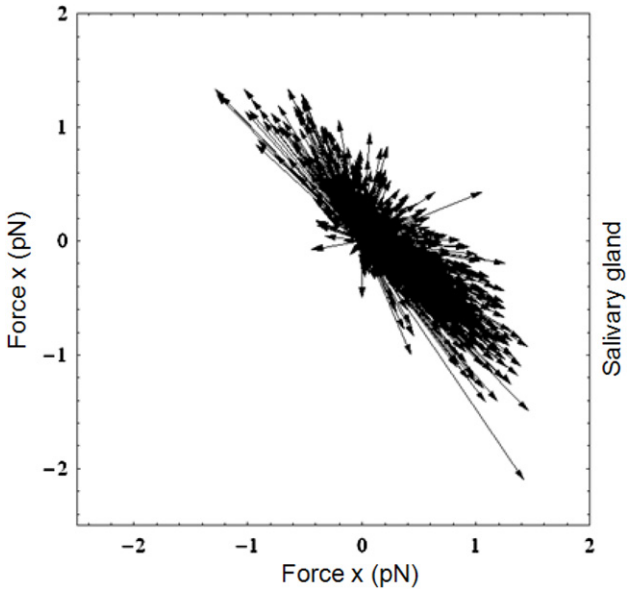

Figure 9. Bidimensional vector force plot of *T. rangeli* in the presence of the salivary gland. The gradient is being generated by all cells.

4. Conclusion

In conclusion, we have developed a methodology to measure in real time the bidimensional vector forces (x and y) of parasites under chemical gradients of concentrations of any kind of chemical substance. Although we have used this system to characterize the chemotaxis process of three specific

protozoa, it could also be used to quantitatively study the taxis of any kind of microorganism under concentration gradients of several chemical substances, as well as in any kind of taxis process related to other types of gradients, such as temperature (thermotaxis), pressure (barotaxis), or osmotic pressure (osmotaxis). We believe that the advantages of the optical tweezers method are: the capability of observing the directionality and strength of the force in real time and the capability of observing the same single biological system behavior under different gradients instead of taking averages over a large number of parasites. We were able to perform the measurements in a high controlled environment, in the case of *L. amazonensis*, and in an environment with the gradient created by living cells, in the case of *T. cruzi*. The investigation of chemotaxis is essential to understand the infection processes, because parasites must recognize and move towards the cells to be infected. This study can help us to understand Chagas disease, Leishmaniasis and other kinds of parasite sickness.

Acknowledgments

The authors are grateful to CAPES, CNPq, FAPESP, L'óreal, Brazilian Academy of Sciences and UNESCO, and IOC-FIOCRUZ. This work is also linked to CEPOF (Optics and Photonics Research Center, FAPESP), the National Institute of Photonics Applied to Cell Biology and the National Institute of Photonics.

References

[1] DPDx—Trypanosomiasis, American. Fact Sheet. Centers for Disease Control (CDC). Retrieved 2008-09-11
[2] WHO, World Health Organization 2002
[3] Grisard E C, Moraes M H, Guarneri A A, Girardi F P, Rodrigues J B, Eger-Mangrich I, Tyler K M and Steindel M 2008 Different serological cross-reactivity of *Trypanosoma rangeli* forms in Trypanosoma cruzi-infected patients sera *Parasites Vectors* **1** 20
[4] Bagorda A and Parent C A 2008 Eukaryotic chemotaxis at a glance *J. Cell Sci.* **121** 2621–4
[5] Teves M E, Guidobaldi H A, Uñates D R, Sanchez R, Miska W, Publicover S J, Morales Garcia A A and Giojalas L C 2009 Molecular mechanism for human sperm chemotaxis mediated by progesterone *PLoS ONE* **4** e8211
[6] Sánchez R, Sepúlveda C, Risopatrón J, Villegas J and Giojalas L C 2010 Human sperm chemotaxis depends on critical levels of reactive oxygen species *Fertil Steril.* **93** 150–3
[7] Wu J Y, Feng L, Park H-T, Havlioglu N, Wen L, Tang H, Bacon K B, Jiang Z-H, Zhang X-C and Rao Y 2001 The neuronal repellent slit inhibits leukocyte chemotaxis induced by chemotactic factors *Nature* **410** 948–52
[8] Zheng M, Sun G, Cai S, Mueller R and Mrowietz U 1999 Significant reduction of T-cell chemotaxis to MCP-1 in patients with primary and metastatic melanoma *Chin. Med. J. (Engl.)* **112** 493–6
[9] Kohidai L 1999 Chemotaxis: the proper physiological response to evaluate phylogeny of signal molecules *Acta Biol. Hung* **50** 375–94
[10] Law A M J and Aitken M D 2005 Continuous-flow capillary assay for measuring bacterial chemotaxis *Appl. Environ. Microbiol.* **71** 3137–43
[11] Khan S, Jain S, Reid G P and Trentham D R 2004 The fast tumble signal in bacterial chemotaxis *Biophys. J.* **86** 4049–58
[12] Neuman K C, Chadd E H, Liou G F, Bergman K and Block S M 1999 Characterization of photodamage to *Escherichia coli* in optical traps *Biophys. J.* **77** 2856–63
[13] Bleul C C, Farzan M, Choe H, Parolin C, Clark-Lewis I, Sodroski J and Springer T A 1996 The lymphocyte chemoattractant SDF-1 is a ligand for LESTR/fusin and blocks HIV-1 entry *Nature* **382** 829–33
[14] Nagasawa T, Hirota S, Tachibana K, Takakura N, Nishikawa S, Kitamura Y, Yoshida N, Kikutani H and Kishimoto T 1996 Defects of B-cell lymphopoiesis and bone-marrow myelopoiesis in mice lacking the CXC chemokine PBSF/SDF-1 *Nature* **382** 635–8
[15] Nelson R D, Quie P G and Simmons R L 1975 Chemotaxis under agarose—new and simple method for measuring chemotaxis and spontaneous migration of human polymorphonuclear leukocytes and monocytes *J. Immunol.* **115** 1650–6
[16] Blair D F 1999 How bacteria sense and swim *Annu. Rev. Microbiol.* **49** 489–522
[17] Rao C V, Glekas G D and Ordal G W 2008 The three adaptation systems of Bacillus subtilis chemotaxis *Trends Microbiol.* **16** 480–7
[18] Barros V C, Oliveira J S, Melo M N and Gontijo N F 2006 *Leishmania amazonensis*: chemotaxic and osmotaxic responses in promastigotes and their probable role in development in the phlebotomine gut *Exp. Parasitol.* **112** 152–7
[19] Pfeffer W 1888 *Unters. Botan. Inst. Tubingen* **2** 582–661
[20] Adler J 1973 A method for measuring chemotaxis and use of the method to determine optimum conditions for chemotaxis by *Escherichia coli J. Gen. Microbiol.* **74** 77–91
[21] Pozzo L Y, Fontes A, de Thomaz A A, Santos B S, Farias P M, Ayres D C, Giorgio S and Cesar C L 2009 Studying taxis in real time using optical tweezers: applications for *Leishmania amazonensis* parasites *Micron* **40** 617–20
[22] Chagas C 1909 Nova tripanosomiase humana *Mem. Inst. Oswaldo Cruz.* **1** 1–62
[23] Nogueira N F S, Garcia E S, Gonzalez M S and De Souza W 1997 Effects of azadirachtin a on the fine structure of the midgut of *Rhodnius prolixus* (Hemiptera: Reduviidae) *J. Invert. Pathol.* **69** 58–63
[24] Gonzalez M S, Hamedi A, Albuquerque-Cunha J M, Nogueira N F S, De Souza W, Ratcliffe N A, Azambuja P, Garcia E S and Mello C B 2006 Antiserum against perimicrovillar membranes and midgut tissue reduces the development of *Trypanosoma cruzi* in the insect vector *Rhodnius prolixus Exp. Parasitol.* **114** 297–304
[25] Alves C R, Albuquerque-Cunha J M, Mello C B, Garcia E S, Nogueira N F, Bourguingnon S C, de Souza W, Azambuja P and Gonzalez M S 2007 *Trypanosoma cruzi*: attachment to perimicrovillar membrane glycoproteins of *Rhodnius prolixus Exp. Parasitol.* **116** 44–52
[26] Gomes S A O, Souza A L F, Kiffer T M, Dick C F, Santos A L A and Meyer-Fernandes J R 2008 Ecto-phosphatase activity on the external surface of *Rhodnius prolixus* salivary glands: modulation by carbohydrates and *Trypanosoma rangeli Acta Trop.* **106** 137–42
[27] Vallejo G A, Guhl F and Schaub G A 2009 Triatominae-*Trypanosoma cruzi/T. rangeli*: vector-parasite interactions *Acta Trop.* **110** 137–47
[28] Happel J and Brenner H 1991 *Low Reynolds Number Hydrodynamics with Special Applications to Particulate Media* (Dordrecht: Klumer)
[29] *Handbook of Chemistry and Physics* 1971 (Cleveland: Chemical Rubber Company)
[30] de Thomaz A A *et al* 2009 Optical tweezers force measurements to study parasites chemotaxis *Proc. SPIE* **7367** 73671A